Analysis of the dispersion properties of a multimode waveguide made of composite polymer for the generation of two-photon quantum states of light

O.A. Ermishev (https://orcid.org/0000-0002-0561-340X)[a,]*, V.K. Boldysheva (https://orcid.org/ 0009-0002-3777-6411) [a], A. I. Garifullin (http://orcid.org/0000-0002-5333-4712) [a,b], N.M. Arslanov (https://orcid.org/ 0000-0001-6651-693X)[a,] **,

[a] *Kazan Quantum Center, Kazan National Research Technical University n.a. A.N. Tupolev – KAI, Kazan, 420111 Russia*

[b] *Institute of Physics, Kazan Federal University, Kazan, 420008 Russia*

**e-mail: oleg22501@mail.ru*

***e-mail: narkis@yandex.ru*

Abstract. The development of a two-photon light field source based on the effect of spontaneous four-wave mixing (SFWM) of light involves solving a number of tasks: from choosing a structure of suitable length and nonlinearity to a detailed analysis of dispersion properties. We consider an integrated spiral waveguide made of a composite polymer using optical lithography as a potential photon pair generation scheme. As a result of the analysis of the modes and dispersion properties, it was possible to determine the zero-dispersion wavelengths necessary for the occurrence of the SFWM effect, as well as the main limitations of the wavelength range of the generated two-photon fields.

Key words: two-photon fields, spontaneous four-wave mixing of light, spiral waveguide, composite polymer, dispersion properties.

INTRODUCTION

The widespread use of photonic quantum technologies in applied fields and the development of a number of systems, such as quantum computers and the quantum Internet, imply a significant increase in the complexity of devices designed to prepare, manipulate and detect quantum states. In this sense, it is most advisable to place all the listed devices and systems on a single technological platform – a photonic integrated circuit. The compactness and scalability of quantum systems produced on a single integrated platform has made the field of integrated quantum technologies one of the most actively developing in recent decades [1, 2].

One of the most important tasks in the field of integrated quantum optics is the creation of an integral source of photon pairs, which implies the development and simplification of technologies for creating structures on new technological platforms [1]. Polymer materials, whose optical and nonlinear properties can be modified, have great prospects in solving this problem [3]. In contrast to optically denser media, where integral structures have compact dimensions and require more complex and expensive manufacturing technology [1], polymer materials make it possible to produce affordable integrated structures due to their relatively large size.

The practical implementation of a two-photon SFWM source based on a multimode microwaveguide assumes knowledge of the linear and nonlinear optical and dispersion properties of polymer waveguides, which depend on the geometry of the waveguide, and, consequently, on the manufacturing technology [1]. Due to the weak third-order nonlinearity of the unmodified

polymer, the length of the waveguide in which generation is to be started should be on the order of tens of centimeters [4, 5, 6], which can only be achieved for a spiral integral structure [5] (Fig.1). If information about the orders of nonlinearity of polymers can be found in a number of sources [7], and the length range of spiral waveguides may well reach the values necessary for high-frequency generation [4,5], then determining the dispersion parameters of waveguides with a certain cross-sectional geometry is a non-trivial task and requires separate calculations [8].

The article presents a numerical analysis of the dispersion properties of an integral waveguide made of a composite polymer in order to identify the influence of the transverse geometry of the waveguide on the dispersion properties and determine the wavelength range with zero dispersion, which is necessary to achieve highly efficient generation of a two-photon field. The waveguides were manufactured using our scientific and educational lithographer, which was created and automated in our laboratory. The characteristics of such a lithographer are not inferior to commercial analogues of the corresponding class (resolution of structures from 0.6 microns and above) and it is possible to debug work, improve automation and supplement equipment depending on the tasks set.

PHASEMATCHING IN NANOWAVEGUIDE SFWM GENERATION

The quantum state of a photon pair arising due to SFWM in a nonlinear nanowaveguide structure is generally described by the following expression [9]:

$$\left|\Psi\right\rangle_{SFWM} = \alpha\left|0\right\rangle + \beta\sum_{klm} A_{klm}\iint d\omega_s d\omega_i f_{klm}(\omega_s,\omega_i)\hat{a}_s^{(l)}(\omega_s)\hat{a}_i^{(m)}(\omega_i)\left|0\right\rangle, \quad (1)$$

where α and β are related to the probabilities of generating the vacuum and two-photon states, respectively. β it also combines all constants related to generation efficiency. The mode composition of interacting fields has a separate effect on the generation. $A_{klm} = \iint dxdy f_p^{(k)}(x,y) f_s^{(l)}(x,y) f_i^{(m)}(x,y)$ – Integral of overlapping modes. The integrand expression includes the joint spectral amplitude function $f_{klm}(\omega_s,\omega_i)$ and the creation operators for the signal $\hat{a}_s^{(l)}(\omega_s)$ and idler $\hat{a}_i^{(m)}(\omega_i)$ photons.

In this paper, we will limit ourselves to the condition that all interacting fields are in the same mode. In this regard, expression (1) will be simplified to the following form [8]:

$$\left|\Psi\right\rangle_{SFWM} = \alpha\left|0\right\rangle + \beta\iint d\omega_s d\omega_i f(\omega_s,\omega_i)\hat{a}_s(\omega_s)\hat{a}_i(\omega_i)\left|0\right\rangle. \quad (2)$$

We are most interested in the spectral properties of the two-photon state associated with to the joint spectral amplitude function:

$$f(\omega_s,\omega_i) \to \alpha(\omega_s+\omega_i) * \phi(\omega_s,\omega_i). \quad (3)$$

In expression (3) $\alpha(\omega_s+\omega_i)$ – the pump spectral distribution, $\phi(\omega_s,\omega_i)$ – the phase-matching function, which in our case has the form:

$$\phi(\omega_s,\omega_i) = \exp\left(\frac{i\Delta\beta L}{2}\right) * \sin c\left(\frac{\Delta\beta L}{2}\right). \quad (4)$$

From expressions (2,4), information can be obtained about the spectrum of the state generated by the SFWM:

$$\Phi \propto \sin c^2\left(\frac{\Delta k L}{2}\right). \quad (5)$$

The argument of the phase-matching function are the length of the nonlinear structure L, which in our case will be fixed, and the wavenumber mismatch $\Delta\beta$, which is defined by the expression to ensure perfect phase-matching:

$$\Delta\beta = 2\beta(\omega_p) - \beta(\omega_s) - \beta(\omega_i) + 2\gamma P_p = 0, \quad (6)$$

where ω_p, $k(\omega_p)$ is the frequency and wavenumber of the pump photon c ω_s, $k(\omega_s)$ is the frequency and wavenumber of the signal photon, ω_i, $k(\omega_i)$ is the frequency and wavenumber of the idle photon. Wavenumber - $\beta(\omega) = \frac{n_{eff}(\omega) * \omega}{c}$, which is related to the effective refractive index of the waveguide structure $n_{eff}(\omega)$. In addition, the phasematching expression contains a term related to the nonlinear properties of the structure, including the pump power and the coefficient of nonlinearity of the structure:

$$\gamma = \frac{n_2 * \omega}{c * A_{eff}}, \quad (7)$$

where A_{eff} - effective mode area, $n_2 = \frac{3 * \chi^{(3)}}{4n_0^2 * c * \varepsilon_0}$ - a nonlinear refractive index, where there is a linear refractive index n_0, a dielectric constant ε_0, and a nonlinearity parameter $\chi^{(3)}$.

In the case of SFWM, phasematching can be achieved either if there is zero dispersion of second-order group velocities at the pump wavelength [8,9], or due to a different mode order [10]. Since in our case all the interacting fields are in the same mode, a method based on zero dispersion will be considered.

When decomposed into a series, expression (4) takes the following form:

$$\Delta\beta = 2\beta(\omega_p) - \beta(\omega_s) - \beta(\omega_i) + 2\gamma P_p = \sum_{n=1}^{\infty} \frac{\beta^{(2n)}}{(2n)!} \Omega^{2n} + 2\gamma P_p, \quad (8)$$

where $\beta^{(2n)} = \frac{d^{2n}}{d\omega^{2n}} \left(\frac{n_{eff}(\omega) * \omega}{c} \right)$ -even-order goup velocity diosprsion.

The most important feature of waveguide and integral structures is the fact that the dependence A is influenced by both the materials from which the fiber core/cladding or waveguide/substrate of the integral structure are made, and the geometry of the cross-section [1,9]. Therefore, when considering an integral waveguide structure with a certain geometry, it becomes possible to determine the wavelength of zero dispersion by modeling, having information about materials and dimensions.

DEVELOPMENT OF A SOFTWARE MODEL OF THE INTEGRATED POLYMER WAVEGUIDE

The software model of the waveguide was built on the basis of micrographs of waveguides of various transverse sizes made on our lithographic installation (Fig.2a-b) for a waveguide with a height of 14 microns with an established technological process. Figures 3a and b show a cross-sectional model of the waveguide under study, indicating the materials and basic geometric parameters: the width of the upper part of the waveguide protrusion (W) and the height of the waveguide (H). Due to the low contrast of the photoresist used, the waveguide has edges in the form of curved slopes. To take this feature into account, the angle of inclination of the walls of the equivalent trapezoidal waveguide (U) was introduced.

The parameter n_{eff} is calculated for a specific geometric structure of the waveguide cross-section by solving a wave equation of the specified form:

$$\Delta E + k_0^2 \mu E = 0, \quad (9)$$

where Δ is the total Laplacian in the coordinates (x,y,z), $\overline{E}(x,y,z) = \widetilde{E}(x,y) * e^{-ik_z z}$, ε, μ is the electric and magnetic permeability, $k_0 = \frac{\omega}{c}$, ω is the frequency of light, c is the speed of light, $\varepsilon \approx n^2$, n is the refractive index of the surface material, and we neglect the losses in the dielectric waveguide.

The calculation was performed in the COMSOL Multiphysics software environment. At the first stage, a wave calculation was performed for the structure under study at a fixed wavelength of the electromagnetic field in order to determine the number of modes that can be supported in the waveguide. Then the method was extended to the entire studied wavelength range of 400-3000 nm. Based on the data obtained, the dispersion properties of the studied modes were calculated.

RESULTS

Figure 4 shows the modes supported in the waveguide at H=4 um, W=10 um and λ=1550 nm. Due to the low contrast of the refractive indices of the waveguide material and the substrate, a micron-sized waveguide is required to maintain a stable mode. The minimum dimensions of the waveguide for a glass substrate, at which the mode will be preserved in it, are at least: H = 3 um, W = 3 um.

The dielectric nature of the waveguide also affects the modes themselves: HE00 (x - polarization), EH00 (y - polarization), HE10 (x - polarization), EH10 (y - polarization). At the same time, transitions between HE and EH modes, as well as hybrid modes, are possible.

The influence of the transverse geometry on the dispersion is most noticeable in the IR wavelength range (Fig.5-7), with the height of the waveguide having the greatest effect (Fig. 7 (c), (d)). In the visible and near-infrared regions of the spectrum, geometry has virtually no effect on dispersion. The dispersion of higher-order HE10 and EH10 modes is more sensitive to any changes in geometry. In addition, in the case of HE10 and EH10 modes, geometry also affects the operating wavelength range, that is, the area in which these modes will be held in the waveguide (Fig.5(a), Fig.6(b), Fig.7(c)). The zero dispersion values required to generate high-frequency signals are in the wavelength range of 1-1.5 um, and the geometry of the waveguide practically does not affect their location. However, in the case of generation of high-frequency waves in higher-order modes, two dispersion zeros appear (Fig.5(b), Fig.6(d), Fig.7(d)), one of which is more strongly influenced by geometry. Thus, the analysis shows that conditions for the generation of two-photon pairs are possible in a rectilinear polymer waveguide. Changes in the transverse geometry of the waveguides can significantly change the conditions for the wavelengths of the generated fields and the generation efficiency. It is important to note that in a multimode waveguide, the dispersion can be affected not only by straight sections, but also by bends. The study of the effect of bends on the dispersion and conditions of photon pair generation is the subject of a separate study and will be conducted in future articles.

CONCLUSIONS

The dispersion data obtained for the polymer waveguide showed extensive possibilities for controlling the dispersion characteristics of light in polymer multimode waveguides and demonstrated the potential for two-photon fields to occur in it: when manufacturing a spiral integral structure and using powerful pumping with a wavelength in the range of 1-1.5 microns, SFWM two-photon generation can be achieved. At the same time, a single-mode mode can be implemented with achieving phasematching by means of zero dispersion, and a multimode mode, where phasematching can be achieved by using higher-order modes for interacting fields.

FUNDING

Theoretical research and computational work were supported by the Ministry of Science and Higher Education of the Russian Federation (Reg. no. NIOKTR 125012300688-6). The material base for the manufacture of prototypes of polymer waveguide structures is sponsored by the program of strategic academic leadership of KNRTU-KAI named after A. N. Tupolev ("PRIORITY 2030"), Reg. no. NIOKTR 125070808154-3.

CONFLICT OF INTEREST

The authors declare that they have no conflicts of interest.

REFERENCES

1. Zhu, D., et al. Integrated photonics on thin-film lithium niobate// Advances in Optics and Photonics. 2021. V.13 (2). P.242-352.
2. Wang, Jianwei, et al. Integrated photonic quantum technologies.// Nature photonics. 2020. V.14(5). P.273-284.
3. Perez, Joaquin, et al. Continuous broadband MWP true-time delay with PbS-PMMA and PbS-SU8 waveguides// IEEE Photonics Technology Letters. 2016. V.28 (15). P.1657-1660.
4. Mingfei Ding et al. High-efficiency four-wave mixing in low-loss silicon photonic spiral waveguides beyond the singlemode regime// Opt. Express. 2022. V.30. P.16362-16373.
5. David Duchesne et al. Supercontinuum generation in a high index doped silica glass spiral waveguide// Opt. Express. 2010. V.18. P.923-930.
6. Paesani, S. et al. Near-ideal spontaneous photon sources in silicon quantum photonics// Nature communications. 2020. V.11(1). P.2505.
7. D'Amore, Franco, et al. Enhancement of PMMA nonlinear optical properties by means of a quinoid molecule// Optical Materials. 2004. V.24 (4). P.661-665.
8. Smirnov M. A. et al. Bright ultra-broadband fiber-based biphoton source //Optics Letters. 2024. V. 49(14). P.3838-3841.
9. Migdall A., Bienfang, Joshua; Polyakov, Sergey; Fan J. Experimental Methods in the Physical Sciences // Experimental Methods in the Physical Sciences. 2013. Vol. 37
10. Lee, K. et al. Visible wavelength polarization entangled photon-pairs using SFWM in nondegenrate spatial modes//International Conference on Information and Communication Technology Convergence (ICTC). 2021. P. 262-264.

FIGURE CAPTIONS

Fig.1 Spiral waveguide made on an optical lithographer

Fig.2 Cross section of a composite polymer waveguide: (a) height 14 um, width 35 um, (b) height 14 um, width 15 um, (c) height 14 um, width 6 um

Fig.3 A software model of a polymer waveguide cross–section: (a) with indication of materials, (b) with indication of dimensions

Fig.4 Waveguide modes at H=4 um, W=10 um, λ=1550 nm.

Fig.5 Effective refractive index and the 2nd order group velocity dispersion for the HE and EH modes shown in Fig.4

Fig.6 Impact of the waveguide widths W on the HE00(x) and HE10(x) modes: (a), (b) on the effective refractive index, (c), (d) on the 2nd order group velocity dispersion

Fig.7 Impact of waveguide heights H on the HE00(x) and HE10(x) modes: (a), (b) on the effective refractive index, (c), (d) on the 2nd order group velocity dispersion

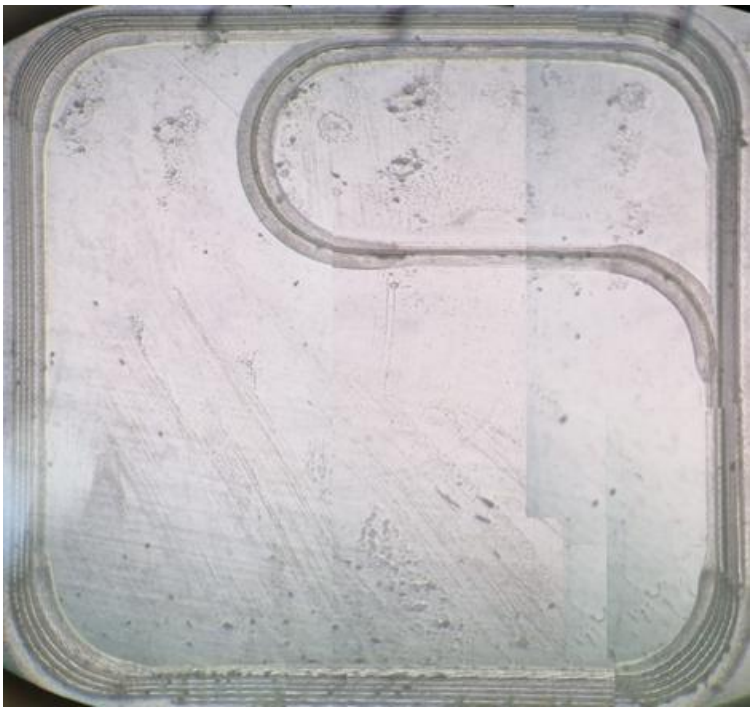

Fig.1

(a) (b) (c)

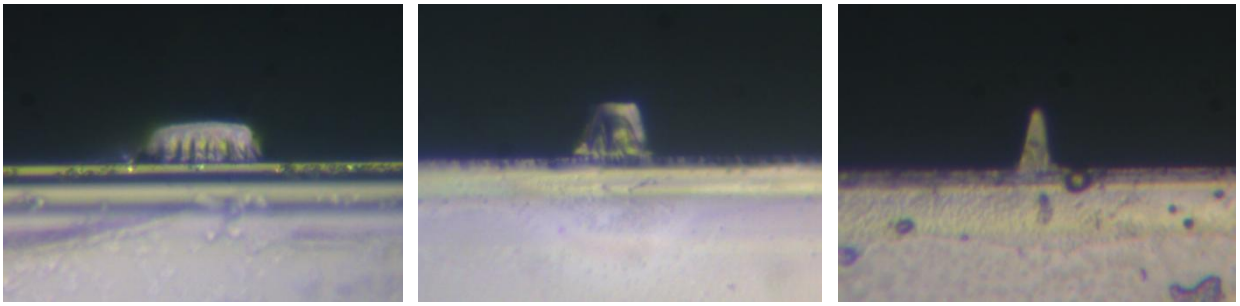

Fig.2

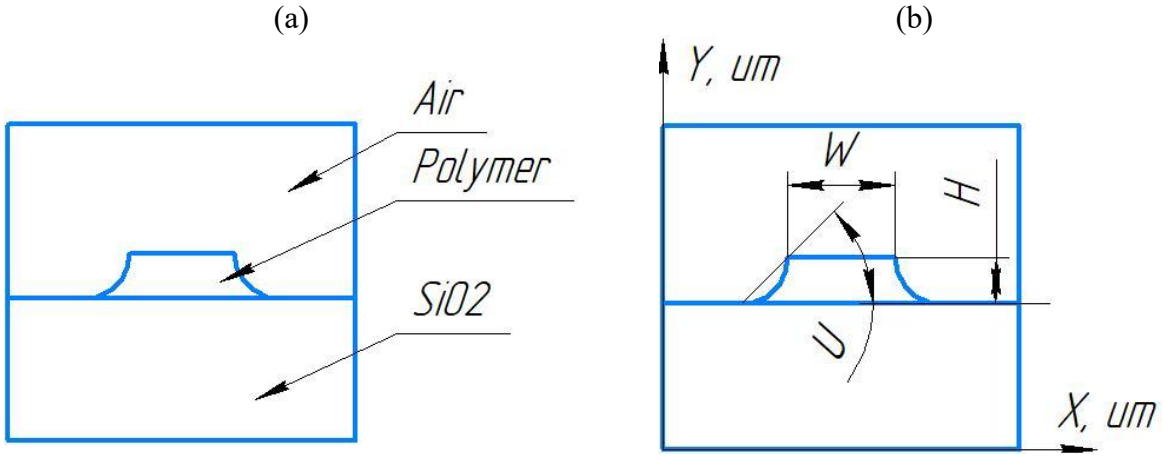
(a)
(b)
Air
Polymer
SiO2
Y, um
W
H
U
X, um

Fig. 3

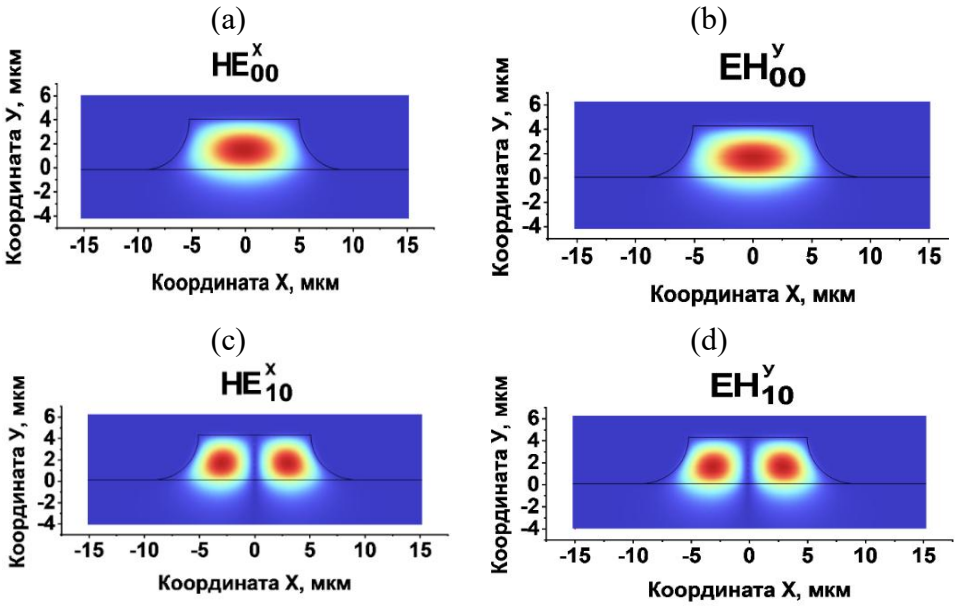
(a)
(b)
(c)
(d)
Координата Y, мкм
Координата X, мкм

Fig.4

(a) (b)

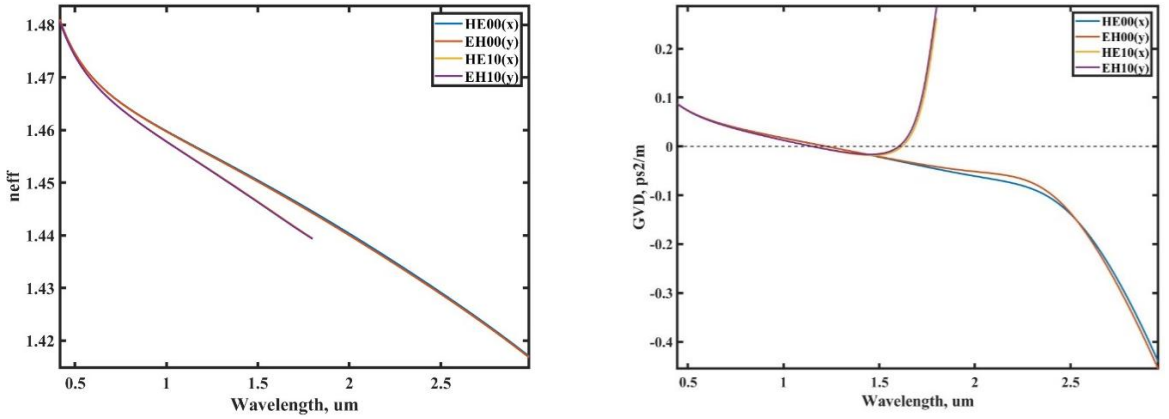

Fig.5

(a) (b)

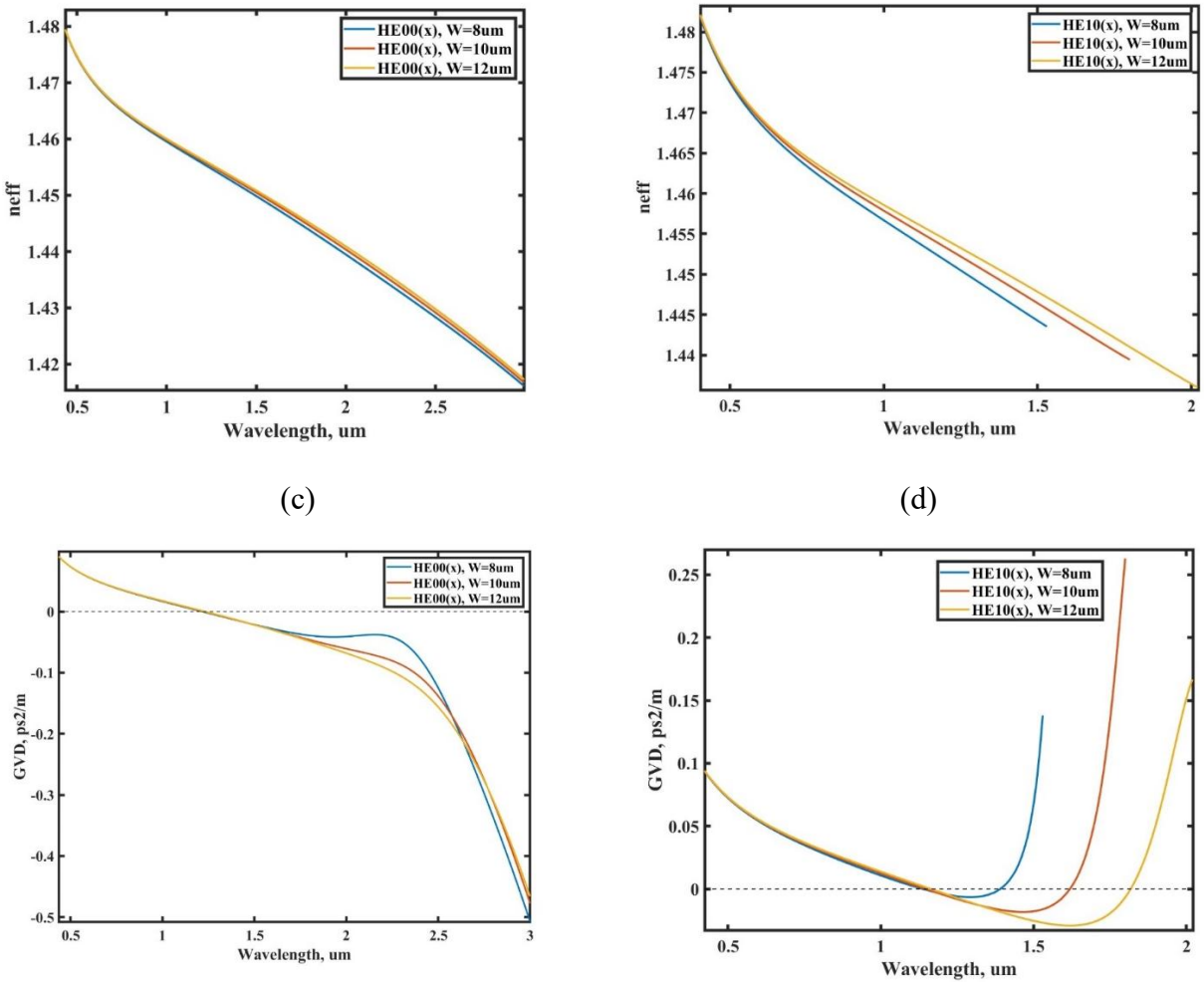

(c) (d)

Fig.6

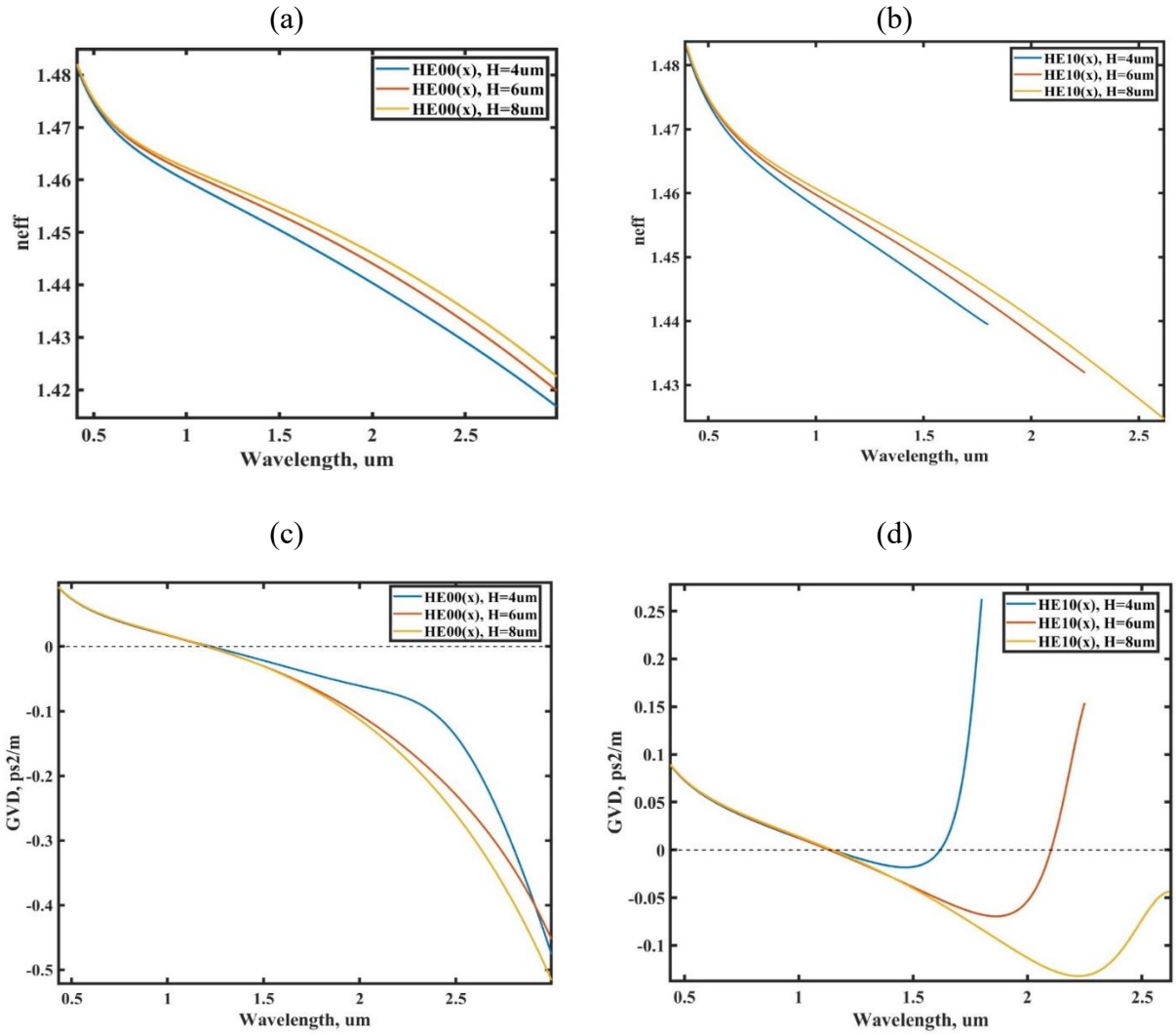
(a)
(b)
(c)
(d)
HE00(x), H=4um
HE00(x), H=6um
HE00(x), H=8um
HE10(x), H=4um
HE10(x), H=6um
HE10(x), H=8um
neff
GVD, ps2/m
Wavelength, um

Fig.7